

***BLIMP1* Is a Tumor Suppressor Gene Frequently Disrupted in Activated B Cell-like Diffuse Large B Cell Lymphoma**

Jonathan Mandelbaum,^{1,2} Govind Bhagat,^{1,3} Hongyan Tang,¹ Tongwei Mo,¹ Manisha Brahmachary,¹ Qiong Shen,¹ Amy Chadburn,⁵ Klaus Rajewsky,⁶ Alexander Tarakhovskiy,⁷ Laura Pasqualucci,^{1,3,8,*} and Riccardo Dalla-Favera^{1,3,4,8,*}

¹Institute for Cancer Genetics and Herbert Irving Comprehensive Cancer Center

²Integrated Program in Cellular, Molecular and Biomedical Studies

³Department of Pathology & Cell Biology

⁴Department of Genetics and Development

Columbia University, New York, NY, 10032, USA

⁵Department of Pathology and Laboratory Medicine, Weill Medical College of Cornell University, New York, NY 10065, USA

⁶Program of Cellular and Molecular Medicine, Children's Hospital, and Immune Disease Institute, Harvard Medical School, Boston, MA 02115, USA

⁷Laboratory of Lymphocyte Signaling, The Rockefeller University, New York, NY 10065, USA

⁸These authors contributed equally to this work

*Correspondence: lp171@columbia.edu (L.P.), rd10@columbia.edu (R.D.-F.)

DOI 10.1016/j.ccr.2010.10.030

SUMMARY

Diffuse large B cell lymphoma (DLBCL) is a heterogeneous disease composed of at least two distinct subtypes: germinal center B cell-like (GCB) and activated B cell-like (ABC) DLBCL. These phenotypic subtypes segregate with largely unique genetic lesions, suggesting the involvement of different pathogenetic mechanisms. In this report we show that the *BLIMP1/PRDM1* gene is inactivated by multiple mechanisms, including homozygous deletions, truncating or missense mutations, and transcriptional repression by constitutively active BCL6, in ~53% of ABC-DLBCL. In vivo, conditional deletion of *Blimp1* in mouse B cells promotes the development of lymphoproliferative disorders recapitulating critical features of the human ABC-DLBCL. These results demonstrate that *BLIMP1* is a bona fide tumor-suppressor gene whose loss contributes to lymphomagenesis by blocking plasma cell differentiation.

INTRODUCTION

Diffuse large B cell lymphoma (DLBCL) represents the most common type of non-Hodgkin's lymphoma in the adult, accounting for ~40% of all diagnoses (Abramson and Shipp, 2005). Based on gene expression profile analysis, distinct DLBCL subtypes have been identified whose transcriptional programs resemble that of normal B cells at various stages of differentiation (Alizadeh et al., 2000; Shaffer et al., 2002a). These include the germinal center B cell-like (GCB) DLBCL, presumably derived from a transformed germinal center (GC) centroblast, and the activated B cell-like (ABC) DLBCL, whose cell of

origin is less clear but may be related to a plasmablastic B cell. A third group of DLBCLs is represented by primary mediastinal large B cell lymphoma, postulated to arise from thymic B cells (Rosenwald et al., 2003; Savage et al., 2003). A separate classification, also based on gene expression profiling, identified three discrete subsets defined by the expression of genes involved in oxidative phosphorylation (OXPHOS), B cell receptor/proliferation (BCR), and tumor microenvironment/host inflammatory response (HR) (Monti et al., 2005).

The subclassification of DLBCL suggests that this disease may in fact comprise several distinct entities utilizing different pathogenetic mechanisms. This notion is supported by the

Significance

ABC-DLBCL, the less curable subtype of DLBCL, has the molecular footprint of a tumor that likely arose from post-germinal center B cells undergoing plasma cell differentiation. Our results show that the pathway controlling terminal differentiation is inactivated in these tumors by a heterogeneous set of mutually exclusive genetic lesions, leading to genetic or epigenetic inactivation of the master plasma cell regulator *BLIMP1*. The observation that conditional B cell deletion of *Blimp1* in the mouse promotes DLBCL with features of human ABC-DLBCL demonstrates that the plasma cell differentiation pathway is critically involved in suppressing lymphomagenesis and provides conclusive evidence for *BLIMP1* as a tumor suppressor. Mice with B cell-specific deletion of *Blimp1* may represent faithful models of preclinical interest for this disease.

observation that multiple genetic lesions of plausible pathogenic significance segregate with different subtypes of DLBCL (Lenz et al., 2008b). With a focus on the ABC/GCB-based classification, it is known that translocations of *BCL2* (Huang et al., 2002), mutations within the *BCL6* autoregulatory domain (Iqbal et al., 2007; Pasqualucci et al., 2003), and mutations of *EZH2* (Morin et al., 2010) are associated with the GCB subtype, whereas *BCL6* translocations (Iqbal et al., 2007; Ye et al., 1993), amplifications of the *BCL2* locus on 18q24 (Iqbal et al., 2004), and mutations within the NF- κ B (*CARD11*, *TNFAIP3/A20*) (Compagno et al., 2009; Lenz et al., 2008a) and B cell receptor signaling (*CD79B*) (Davis et al., 2010) pathways segregate with the ABC subtype.

Additionally, inactivating mutations of *PRDM1/BLIMP1* have been found exclusively in the ABC subtype (~24% of cases) (Pasqualucci et al., 2006; Tam et al., 2006), although the precise mechanism by which these lesions contribute to lymphoma development has not yet been fully elucidated. *BLIMP1* encodes a transcriptional repressor that is essential for the terminal differentiation of all B cells into plasma cells, as demonstrated by the fact that B cell conditional knockout mice fail to produce plasma cells and serum immunoglobulins (Shapiro-Shelef et al., 2003). *BLIMP1* is thought to promote terminal differentiation in part by repressing genes important in B cell receptor signaling and cellular proliferation (Lin et al., 1997; Shaffer et al., 2002b). Our initial study also reported rare missense mutations of the *BLIMP1* gene, but their functional consequences were not addressed. Furthermore, the majority of ABC-DLBCL studied (~77%) did not express the *BLIMP1* protein despite the presence of IRF4, a transcriptional repressor that is known to be invariably coexpressed with *BLIMP1* in normal GC B cells and in all plasma cells (Angelin-Duclos et al., 2000), suggesting that mechanisms alternative to mutations may be contributing to the lack of protein expression in ABC-DLBCL. Finally, in vivo evidence establishing a direct link between *BLIMP1* inactivation and lymphomagenesis has yet to be reported.

In the present study we investigated the full spectrum of *BLIMP1* lesions by comprehensively characterizing a large panel of DLBCLs for the presence of mutations, copy number alterations, and expression of the *BLIMP1* protein. We analyzed the functional consequences of the *BLIMP1* missense mutations and explored additional epigenetic mechanisms to inactivate *BLIMP1* in ABC-DLBCL. Finally, we assessed the contribution of *BLIMP1* inactivation to the pathogenesis of ABC-DLBCL in vivo.

RESULTS

Inactivation of *BLIMP1* by Truncating Mutations and Biallelic Gene Deletions in DLBCL

To investigate the full complement of genetic lesions affecting *BLIMP1* in DLBCL, we characterized 158 DLBCL samples (139 primary biopsies and 19 cell lines) representative of the major phenotypic subtypes for the presence of mutations and copy number changes affecting the *BLIMP1* gene. The study panel included 51 ABC, 61 GCB, and 10 unclassified DLBCLs, as determined by gene expression profile analysis. The remaining 36 cases were classified by immunohistochemistry into GC (n = 12) and non-GC type (n = 24) (Hans et al., 2004).

Sequencing analysis of the *BLIMP1* coding exons identified 18 truncating mutations in 16 biopsies and 2 cell lines, including frameshift insertions and deletions (n = 11), splice site mutations (n = 6), and one nonsense mutation. Most of the changes clustered toward the N-terminal portion of the *BLIMP1* protein and were predicted by sequence analysis to inactivate protein function by removing critical functional domains, including the PR, proline-rich, and DNA-binding Zinc finger domains (Figure 1A). Consistent with initial reports (Pasqualucci et al., 2006; Tam et al., 2006), all of these mutations were found in cases displaying an ABC/NC (n = 14/51, 27%) or non-GC (n = 4/24, 17%) phenotype, indicating that genetic inactivation of *BLIMP1* is specific for this DLBCL subtype (Figure 1B). Analysis of 6q21 deletions, examined by a combination of copy number analyses, revealed that the majority of the mutated cases (n = 16/18, 89%) had lost expression of the wild-type allele due to deletion, epigenetic silencing, or uniparental disomy of the mutated allele, demonstrating biallelic inactivation of the gene (see Table S1 and Figure S1 available online). Moreover, three ABC-DLBCL cases were found to harbor biallelic gene deletions of 21 Mb, 742 Kb, and 271 Kb, with the latter only encompassing *BLIMP1*, but not the two proximal genes *ATG5* and *PREP* (Figure 1C). This finding provides direct evidence that *BLIMP1* is a critical target gene in the 6q21-deleted region commonly observed in DLBCL (Gaidano et al., 1992).

Missense Mutations Affect *BLIMP1* Protein Stability and Its Trans-Repression Activity

In seven additional cases (five ABC/non-GC and two GCB/GC DLBCLs), we uncovered missense mutations affecting various residues along the entire *BLIMP1* protein (Figure 2A) and associated with loss of the second allele in three cases (Table S2). Sequencing analysis of matched normal DNA in one sample with available material demonstrated the somatic origin of the mutation (Figure S1). The remaining variants were not found in public SNP databases (see Experimental Procedures), with one exception (Y345H), which was, therefore, excluded from the calculation of the mutation frequency.

In order to test the functional significance of these mutations, we first assessed the basal expression levels of the corresponding alleles upon transient transfection in 293T cells. As shown in Figure 2B, three ABC/non-GC DLBCL mutants (P48T, P48R, and Y149D) were expressed at significantly lower protein levels compared to wild-type *BLIMP1*, despite similar mRNA levels, suggesting that these mutations may destabilize the *BLIMP1* protein. Treatment with cycloheximide documented that the proteins encoded by these three mutants had a significantly decreased half-life, with the P48R polypeptide being most unstable (Figure 2C). Accordingly, the Polyphen algorithm (Sunyaev et al., 2001), used to make in silico predictions of the potential functional consequences of missense mutations, determined that these three mutations may affect the *BLIMP1* protein structure and/or folding (data not shown). Furthermore, the SUDHL2 ABC-DLBCL cell line, which harbors the P48R mutation, expresses significantly reduced *BLIMP1* protein levels despite elevated amounts of mRNA (comparable to the multiple myeloma cell line U266) (Figure S2), consistent with protein instability.

We then assessed the relative transrepression activity of the mutant proteins by measuring their ability to downregulate the

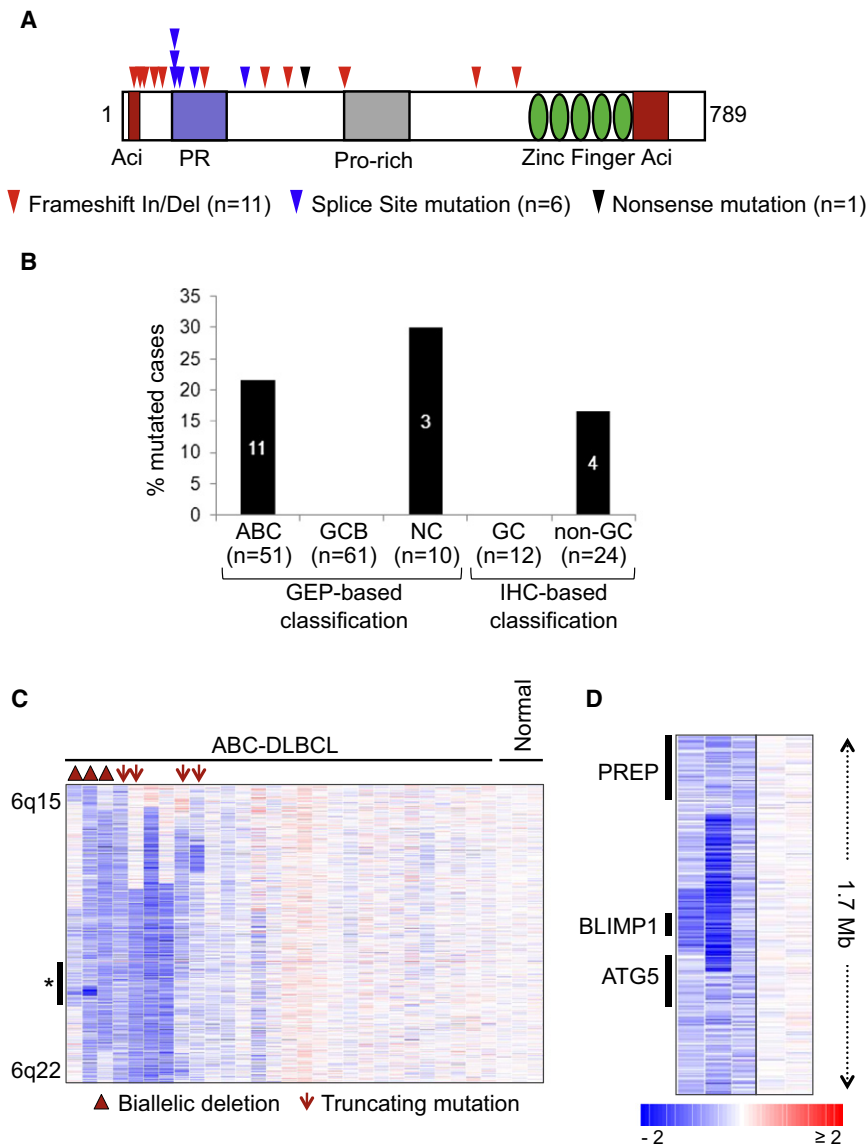


Figure 1. Inactivation of *BLIMP1* by Truncating Mutations and Biallelic Deletions in ABC-DLBCL

(A) Distribution of truncating mutations along the *BLIMP1* protein, with known functional domains annotated. Aci, acidic domain; PR, PR domain; Pro-rich, proline-rich domain (see also Table S1). (B) Percentage of cases with truncating *BLIMP1* mutations in various DLBCL subtypes classified by gene expression profiling (GEP) or by immunohistochemistry (IHC) (see text).

(C) dChip SNP inferred copy number heatmap of the 6q15-q22.1 region in ABC-DLBCL cases and three normal DNA controls. Cases harboring homozygous deletions or truncating mutations are denoted by symbols (see also Figure S1). The region indicated by an asterisk is shown at higher magnification in (D) for the three homozygously deleted cases (and two normal DNAs), with the approximate position of the *BLIMP1*, *ATG5*, and *PREP* genes on the left.

To further investigate the consequences of these mutations in B cells, we overexpressed the mutant alleles in the GCB-DLBCL cell line BJAB via lentiviral-mediated transduction. Compared to empty vector-transduced cells, those infected with wild-type *BLIMP1* failed to proliferate (Figure 3A), consistent with the previously reported ability of *BLIMP1* to repress multiple genes involved in cell cycle progression (Lin et al., 1997; Shaffer et al., 2002b). On the contrary, cells infected with vectors expressing either unstable (P48R, Y149D) or transrepression defective (C569Y) missense mutants proliferated at rates similar to those of control cells. Flow cytometric analysis of the cell cycle profile revealed a 3-fold increase in the G0/G1 population of cells expressing wild-type *BLIMP1*, but not in

expression of a luciferase reporter gene driven by a portion of the *CIITA* gene promoter, a known *BLIMP1* direct target (Piskurich et al., 2000). Compared to wild type, two mutants (P48R, C569Y) failed to efficiently repress the reporter (Figure 2D). In the P48R mutant this effect can be attributed to the observed protein instability and consequently reduced expression levels; however, the C569Y mutant had lost its activity despite comparable protein amounts, suggesting that this mutation may directly impair the *BLIMP1* transrepression function. Indeed, this mutation substitutes a critical cysteine within the second zinc finger of the *BLIMP1* DNA-binding domain, and abrogated DNA binding to the endogenous *CIITA* gene promoter, as assessed in B cells by chromatin immunoprecipitation assays (Figure S2). Overall, these results indicate that a subset of *BLIMP1* missense mutants, specifically those associated with ABC/non-GC DLBCL, impairs the stability and/or function of the *BLIMP1* protein.

cells transduced with the above three mutants (Figure 3B), further documenting their loss of function.

Consistent with results obtained in the previous assays, the P48R, Y149D, and C569Y mutants were also unable to repress the expression of endogenous *ID3* and *CIITA*, two known direct target genes of *BLIMP1* (Shaffer et al., 2002b) (Figure 3C). Interestingly, when compared to cells transduced with wild-type *BLIMP1* or other functionally active mutants, cells expressing these three proteins showed consistently higher levels of GFP, which is coregulated with *BLIMP1* via the bicistronic lentiviral cassette, suggesting counter-selection against high, toxic levels of wild-type *BLIMP1* but not against the functionally deficient mutants (Figure S3).

Finally, we assessed the ability of the various missense mutants to promote plasma cell differentiation, the primary physiological function of *BLIMP1* in B cells. To address this question we utilized *Blimp1* conditional-knockout mouse B cells (*Blimp1*^{CD19KO}), which are unable to undergo plasma cell

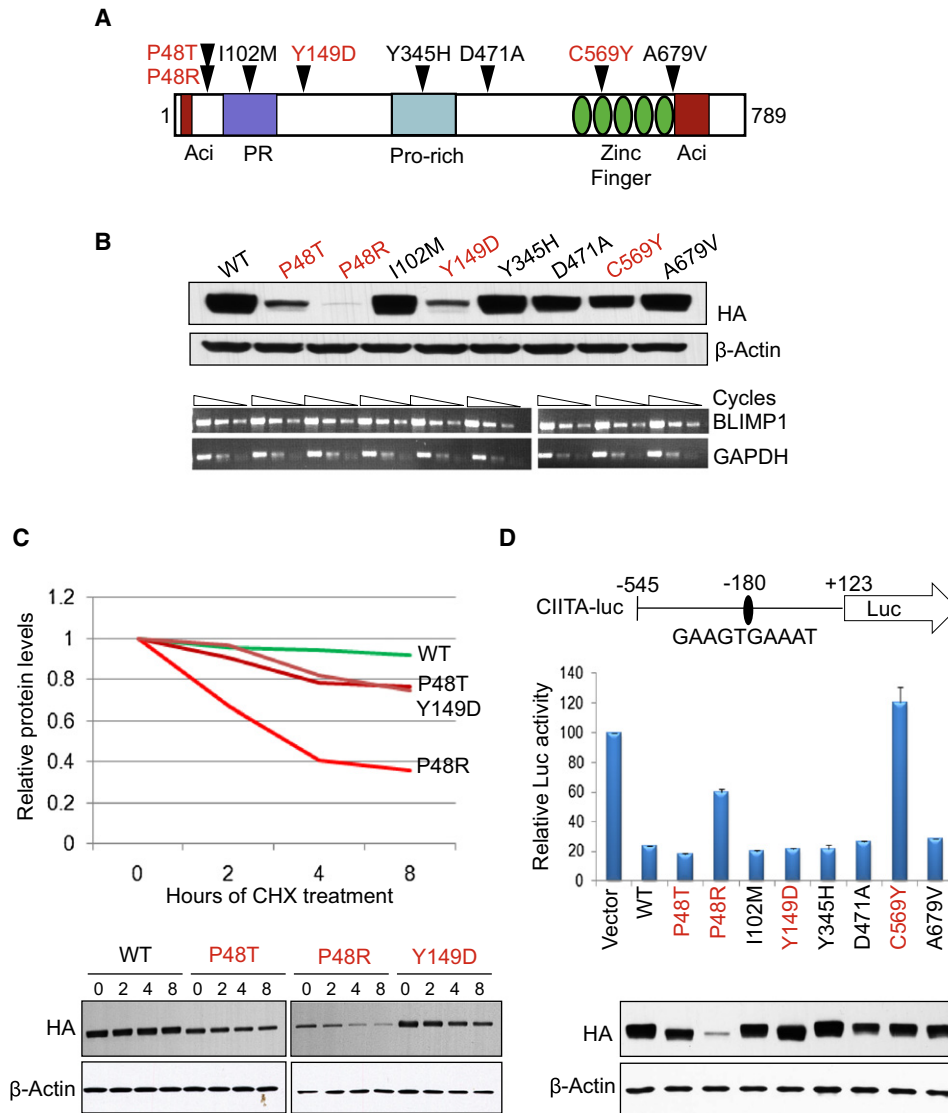


Figure 2. Missense Mutations Affect BLIMP1 Protein Stability and Trans-Repression Activity

(A) Distribution of missense mutations along the BLIMP1 protein; in red, mutants that showed an effect in any of the assays performed in (B)–(D) (see also Table S2).

(B) Western blot (top) and semiquantitative RT-PCR (bottom) analysis of exogenous *BLIMP1* expression in 293T cells transfected with equimolar amounts of vectors expressing HA-tagged wild-type or mutant *BLIMP1* alleles.

(C) Analysis of exogenous BLIMP1 protein expression in 293T cells transfected with the indicated mutant alleles and treated with cycloheximide for 2, 4, or 8 hr. Data were quantitated by densitometric analysis, normalized to β -actin levels, and graphed relative to time zero (top). The Western blot analysis is shown on the bottom panel.

(D) Transrepression activity of wild-type and mutant BLIMP1 proteins in 293T cells cotransfected with a luciferase reporter construct driven by the human *CIITA* promoter (region –545 to +123, encompassing a consensus BLIMP1 binding site at position –180) (top). Luciferase activities are represented as percent change relative to the basal activity of the reporter (set to 100), after normalization to Renilla luciferase activity (mean \pm SD, as obtained from three independent experiments). In the bottom panel, Western blot analysis using anti-HA antibodies monitors for the corresponding exogenous BLIMP1 expression levels; note that for the three unstable mutants, higher amounts of plasmid DNA were transfected to achieve comparable levels. Nevertheless, expression of the P48R mutant protein remained significantly lower than wild type, presumably due to its marked instability (see also Figure S2).

differentiation after stimulation with lipopolysaccharide but can be rescued by retroviral-mediated delivery of wild-type BLIMP1 (Shapiro-Shelef et al., 2003). In this system approximately 10% of the cells reconstituted with wild-type BLIMP1 efficiently differentiated into CD138⁺B220^{lo} plasma cells, analogous to control cells isolated from wild-type animals (12%) (Figure 3D).

Conversely, plasma cell differentiation was significantly reduced in cells reconstituted with the P48R and C569Y mutants (5% and 2%, respectively). The Y149D mutant, which was defective in previous assays, appeared to retain its activity in this system, likely due to the fact that sufficiently high protein levels were achieved via retroviral overexpression (data not shown).

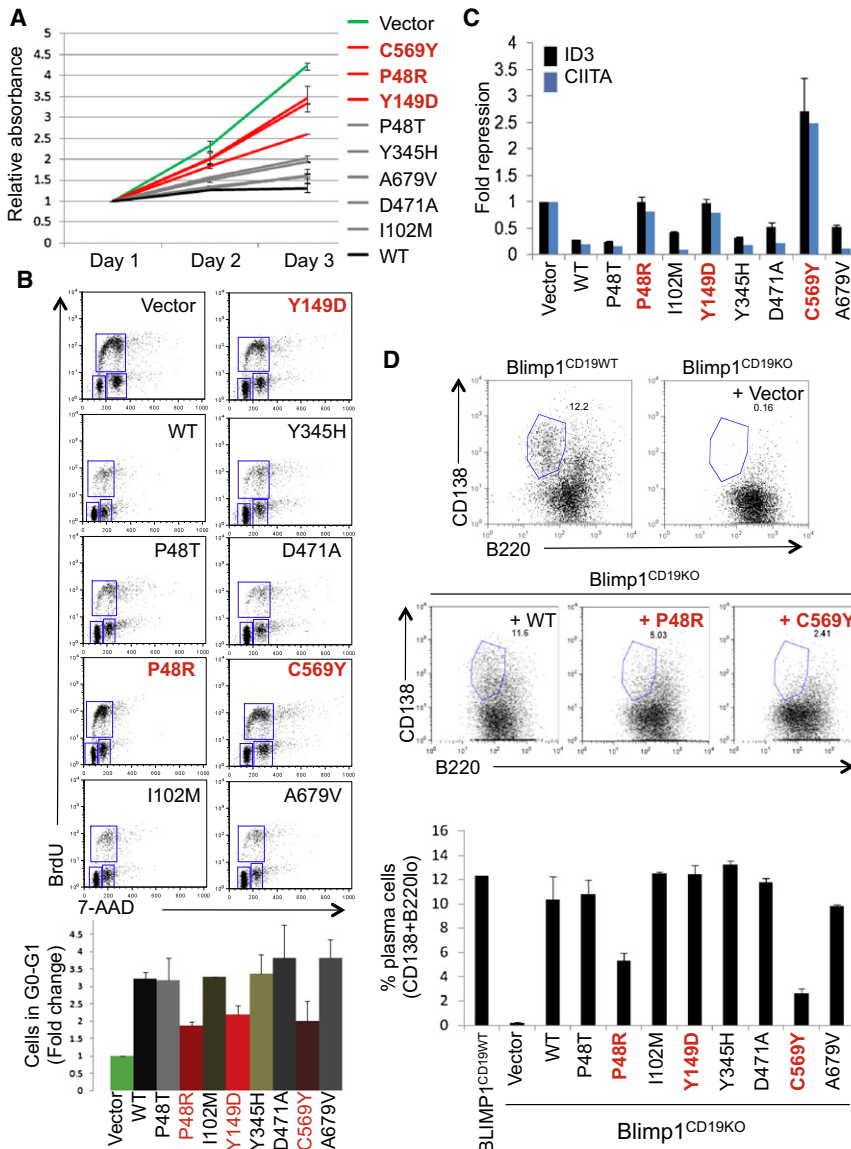


Figure 3. BLIMP1 Missense Mutations Impair Its Ability to Induce Cell Cycle Arrest and Promote Plasma Cell Differentiation

(A) Proliferative capacity of BJAB B cells transduced with lentiviral vectors expressing the indicated BLIMP1 proteins along with GFP, as assessed by an MTT assay on sorted GFP⁺ cells. Shown are representative data from one of two independent experiments performed in duplicate (mean ± SD) (see also Figure S3).

(B) The left side is the representative flow cytometric analysis of BJAB B cells transduced with the indicated vectors and stained for incorporated BrdU and 7-amino-actinomycin D (7-AAD). Region gates define cells residing in G0–G1, S, and G2–M phases of the cell cycle. The G0–G1 population was quantitated relative to empty vector-transduced cells (set at 1), and the mean ± SD from two independent experiments is shown below.

(C) Expression of the BLIMP1 targets *ID3* and *CIITA* in sorted GFP⁺ BJAB B cells, as determined by quantitative real-time RT-PCR (n = 3; mean ± SD). Levels were normalized to both *BLIMP1* and *GAPDH* and are shown as fold changes relative to vector-transduced cells (set as 1).

(D) Representative flow cytometric analysis of CD138 and B220 staining in *Blimp1*^{CD19KO} splenic B cells, reconstituted with the indicated vectors and stimulated to undergo plasma cell differentiation by LPS treatment for 3 days, as compared to wild-type (*Blimp1*^{CD19WT}) B cells. The percentage of cells in the gated (plasma cell) population is shown. Data from two independent experiments are quantitated in the bottom panel (mean ± SD). Mutants that showed an effect in any of the assays (A–D) are indicated in red.

In summary, data from a variety of assays in both 293T and B cells demonstrate that four of the seven somatic missense mutants analyzed displayed functional defects, ranging in their severity from a complete loss of multiple functions (P48R and C569Y) to more subtle effects (P48T and Y149D). Notably, the defective mutants were all associated with ABC/non-GC DLBCL cases.

Epigenetic Inactivation of *BLIMP1* in ABC-DLBCL Cases Carrying *BCL6* Translocations

Taking together cases with functionally deficient missense mutants and cases with truncating mutations and biallelic deletions, our data demonstrate that *BLIMP1* is genetically inactivated in approximately one-third of ABC-DLBCLs (n = 16/51). Nonetheless, additional mechanisms appeared to be contributing to *BLIMP1* inactivation in this tumor subtype because an even larger fraction of cases (n = 27/51, 53%) lacked *BLIMP1* protein expression despite the absence of *BLIMP1* structural

alterations and the presence of IRF4, a protein invariably coexpressed with *BLIMP1* in a subset of normal human GC B cells (Angelin-Duclos et al., 2000) and involved in the terminal differentiation pathway leading to *BLIMP1* activation (Klein et al., 2006; Saito et al., 2007) (Figures 4A and 4B). Given that the *BCL6* transcriptional repressor can directly repress *BLIMP1* expression (Tunyaplin et al., 2004) and is deregulated by chromosomal translocations preferentially in ABC-DLBCL (Ye et al., 1995), we assessed the relationship between structural alterations of *BCL6* and *BLIMP1*. Notably, ~26% (n = 13/51) of ABC-DLBCL cases contained translocations of *BCL6* that were, with two exceptions, mutually exclusive with *BLIMP1* structural alterations (Figure 4C). Cases with *BCL6* translocations also had significantly lower *BLIMP1* mRNA levels compared to cases that lacked translocations and expressed the *BLIMP1* protein (Figure S4). Furthermore, shRNA-mediated knockdown of *BCL6* expression in the *BCL6*-translocated RCK8 and OCI-Ly8 ABC/non-GC-DLBCL cell lines promoted upregulation of *BLIMP1* mRNA and protein (Figure 4D; data not shown). Overall, these data support the hypothesis that deregulated *BCL6* expression via chromosomal translocations is responsible for suppressing *BLIMP1*

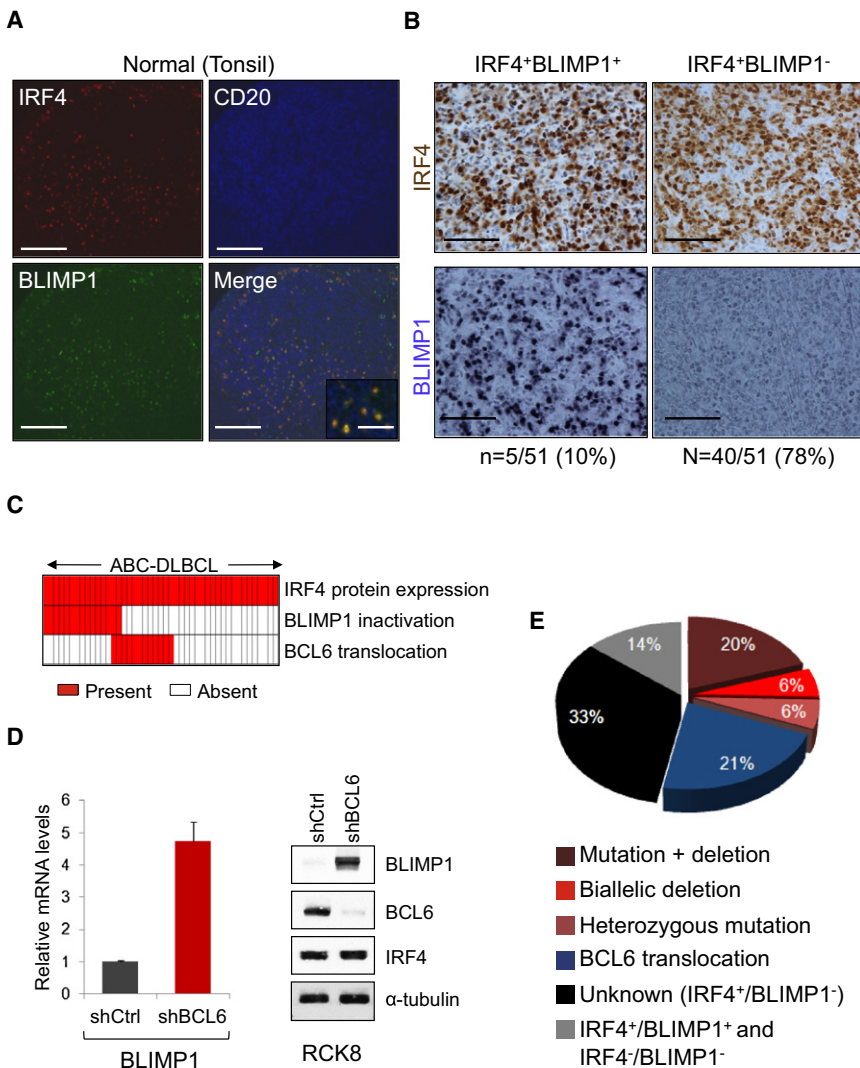


Figure 4. BCL6 Translocations and BLIMP1 Inactivation Are Mutually Exclusive in ABC-DLBCL

(A) Immunofluorescence analysis of BLIMP1 (green), IRF4 (red), and CD20 (blue) expression in normal GC cells of a human tonsil (scale bar, 325 μ m; inset, 150 μ m).

(B) IRF4 (brown) and BLIMP1 (blue) immunostaining in representative ABC-DLBCL cases displaying a normal expression pattern (IRF4⁺BLIMP1⁺) (left panels) or specific lack of BLIMP1 expression (IRF4⁺BLIMP1⁻) (right panels) (scale bar, 125 μ m). The percentage of cases in each group is provided below. Six additional cases (12%) were negative for expression of both proteins (not shown; see also Tables S1 and S2 for a detailed characterization of individual cases).

(C) Distribution of BLIMP1 and BCL6 structural alterations in IRF4+ ABC-DLBCL. Columns represent individual patients, with color codes indicating the presence or absence of the corresponding feature.

(D) BLIMP1 mRNA (left) and protein (right) levels in the BCL6-translocated RCK8 cell line, transduced with lentiviral vectors expressing a control shRNA (shCtrl) or a BCL6-specific shRNA (shBCL6). BLIMP1 mRNA levels were determined by quantitative real-time RT-PCR and are shown as fold change relative to shCtrl-transduced cells, after normalization for GAPDH (n = 3; mean \pm SD). Western blot analysis of BCL6 controls for efficient BCL6 knockdown (see also Figure S4).

(E) Overall frequency of BLIMP1 and BCL6 structural alterations in ABC-DLBCL. The unknown category denotes cases that lack BLIMP1 protein expression, in the absence of BLIMP1 or BCL6 structural alterations. Two cases carrying both BCL6 translocations and biallelic BLIMP1 inactivation were included into the "BLIMP1 mutation + deletion" category.

expression in a fraction of IRF4⁺ ABC-DLBCLs. Thus, over half (53%, n = 27/51) of these tumors have inactivated BLIMP1 through predominantly mutually exclusive structural alterations of BLIMP1 and BCL6 (Figure 4E).

Conditional Deletion of Blimp1 in the Mouse Results in the Development of B Cell Lymphoproliferative Disorders and DLBCL

To assess the role of BLIMP1 inactivation in lymphomagenesis in vivo, we generated mice lacking Blimp1 specifically in B cells by crossing Blimp1 conditional-knockout mice (Ohinata et al., 2005) with CD19-Cre (Rickert et al., 1997) or C γ 1-Cre (Casola et al., 2006) mice, leading to deletion of Blimp1 in all B cells (Blimp1^{CD19KO}) or GC B cells (Blimp1^{C γ 1KO}), respectively. Consistent with previous data (Shapiro-Shelef et al., 2003), Blimp1^{CD19KO} B cells failed to differentiate into immunoglobulin-secreting plasma cells, both in vivo and after ex vivo stimulation (Figure S5; data not shown). On the contrary, immunized Blimp1^{C γ 1KO} mice had selective impairment in GC-derived

IgG1, but not in IgM production, consistent with a specific block in GC-dependent plasma cell differentiation (Figure S5). The Blimp1^{CD19KO} mice also showed a significant increase of the fraction of B220⁺PNA^{hi} GC B cells and CD21⁺CD23⁻ extra-follicular marginal zone (MZ) B cells (Figure 5A). Although we cannot formally exclude that a decrease in the CD23⁺CD21⁻ follicular (FO) B cell compartment can contribute to the increase in the MZ B cell fraction, the observation that FO B cell development is normal in an analogous Blimp1 knockout model (Shapiro-Shelef et al., 2003) suggests that the accumulation of both GC and MZ B cells is due to a block in terminal B cell differentiation.

Macroscopic examination of animals sacrificed between 10 and 16 months of age showed the presence of splenomegaly, suggestive of lymphoproliferation, in most Blimp1^{CD19KO} mice (90%, n = 34/38) (Figure 5B). Subsequent histological examination of the lymphoid organs revealed that ~68% (n = 26/38) of the animals had developed a variety of lymphoproliferative disorders, including MZ B cell hyperplasia (MZBCH; n = 14), characterized by the expansion of small cells surrounding the B cell

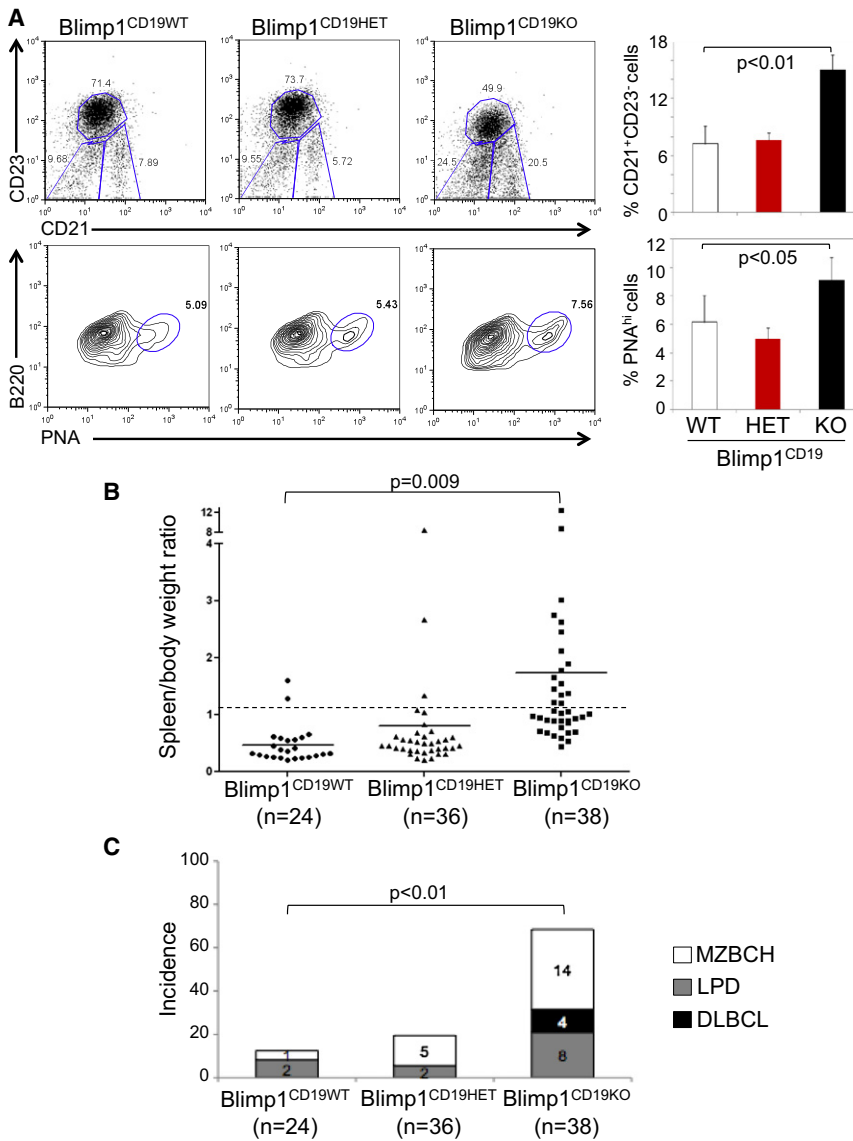


Figure 5. *Blimp1* B Cell Conditional Knockout Mice Develop Lymphoproliferative Disorders

(A) Representative flow cytometric analysis of splenic B cell suspensions isolated from mice of the indicated genotypes and stained for CD21/CD23 (top) and B220/PNA (bottom). A significant increase in both GC (B220⁺PNA^{hi}) and extra-follicular, MZ (CD21⁺CD23⁻) B cell subpopulations can be seen in the *Blimp1*^{CD19KO} animals, as compared to their control littermates. Data are quantitated on the right (mean ± SD; n = 3).

(B) Spleen/body weight ratio in mice of the indicated genotypes, analyzed between 10 and 16 months of age. Splenomegaly was defined as an increase in the spleen/body weight ratio above 0.7% (dashed line). Solid lines indicate the mean value in each genotype.

(C) Frequency of lymphoproliferative disorders in the three cohorts shown in (B). p values (Student's t test) are provided if significant (<0.05). See also Figure S5 and Table S3.

between 12 and 18 months of age, *Blimp1*^{Cγ1KO} mice did not show splenomegaly nor increased incidence of MZBCH, yet they developed LPD and DLBCL at similar penetrance with respect to the *Blimp1*^{CD19KO} model (Figure 6B), demonstrating that deletion of *Blimp1* in the GC alone was sufficient to promote lymphomagenesis.

In both models, the majority of the DLBCLs were Irf4 positive (86%, n = 6/7) (Figure 7) and negative for GC and differentiation markers (i.e., Bcl6, PNA and CD138) (Figure S6B), consistent with the phenotype of a post-GC, activated, preplasmablastic B cell (Falini et al., 2000). Interestingly, these tumors also displayed nuclear NF-κB p50 (Figure 7) indicative of constitutive NF-κB activation, as observed in human ABC-DLBCL (Davis

et al., 2001). Sequencing analysis of three common targets of genetic lesions associated with constitutive NF-κB activity in the human disease (*Tnfrsf3/A20*, *Card11*, and *Cd79b*) did not reveal the presence of mutations in six DLBCL cases analyzed (data not shown), suggesting that constitutive NF-κB activation is necessary for ABC-DLBCL pathogenesis but is induced by different mechanisms in this model.

Over time, *Blimp1*^{CD19KO} mice showed significantly reduced survival, such that at 15 months of age, only 20% of the animals were still alive (Figure S6C). Interestingly, the majority of these mice had an expansion of the bronchus-associated lymphoid tissue (BALT) (79%, n = 30/38) consistent with the diagnosis of BALT hyperplasia (BALT-H), in the presence (n = 21/30) or absence (n = 9/30) of other lymphoproliferative disorders (Figure S6D). Immunostaining of the BALT-H demonstrated an expansion of both Pax5⁺ B cells and CD3⁺T cells within a relatively preserved B-T cell architecture (Figure S6E), suggestive of

follicles; lymphoproliferative disease (LPD) (n = 8), defined by the initial obliteration of the follicular architecture; and DLBCL (n = 4), characterized by a complete effacement of the tissue architecture due to infiltrating large cells (Figures 5C and 7). These disorders were of B cell origin because they stained positive for the pan-B cell marker B220 (Figure 7). Furthermore, analysis of the rearranged Ig genes demonstrated a clonal origin of the disease in all DLBCLs and LPDs tested, as well as in 5/14 (36%) MZBCHs (Figure S6A). Most of the clonal lymphoproliferations carried somatically hypermutated immunoglobulin genes (71%, n = 10/14), documenting the tumor derivation from a cell that had transited the GC (Table S3).

Similar to the *Blimp1*^{CD19KO} mice, *Blimp1*^{Cγ1KO} mice showed a 2-fold increase in the proportion of GC B cells after immunization (Figure 6A). However, these animals did not display an increase in the MZ B cell compartment, consistent with the restriction of *Blimp1* deletion to GC B cells. When analyzed

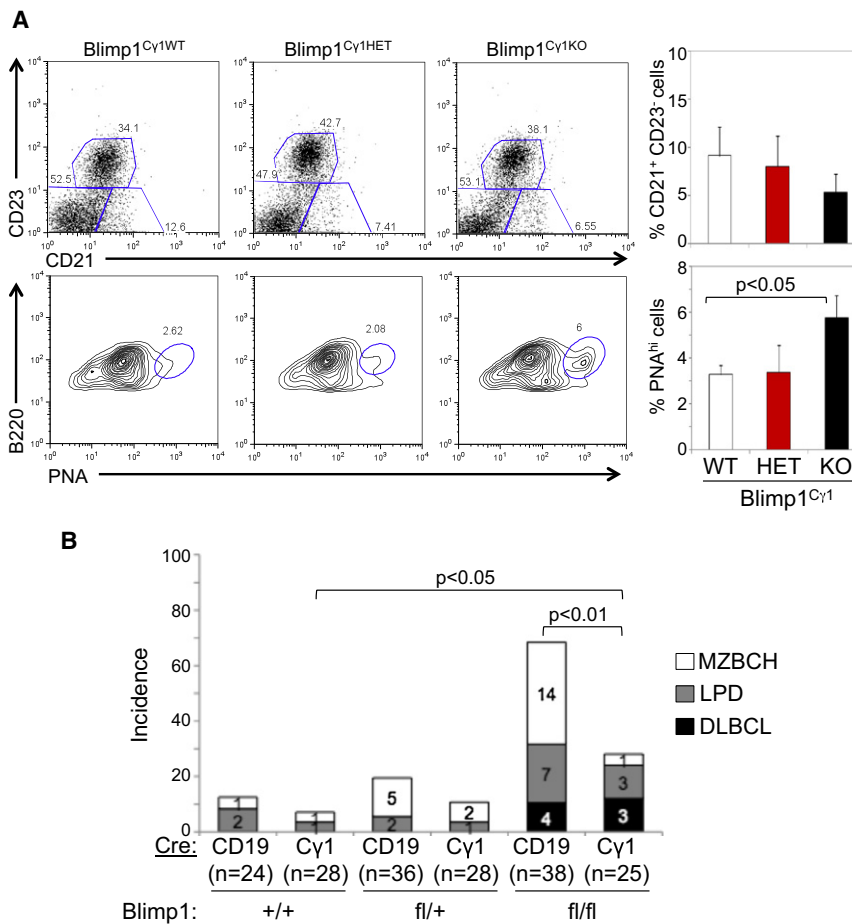


Figure 6. Conditional Deletion of *Blimp1* in the GC Promotes Lymphomagenesis

(A) Representative flow cytometric analysis of the CD21⁺CD23⁻ MZ B cell and B220⁺PNA^{hi} GC B cell compartments in mice of the indicated genotypes, analyzed 10 days after SRBC immunization (left). Data from three mice per genotype are quantitated on the right (mean ± SD).

(B) Percentage of mice developing lymphoproliferative disorders in the CD19-Cre and Cγ1-Cre models, sacrificed between 10 and 18 months of age. See also Table S4.

lesions will likely contribute to lymphomagenesis through additional, distinct mechanisms. This possibility is supported by the fact that the *IμHABCL6* mouse model of DLBCL does not phenocopy the *Blimp1* conditional-knockout mouse model as the *IμHABCL6* mice have both an increased incidence and heterogeneity of DLBCL (Cattoretti et al., 2005). Because BCL6 is known to regulate multiple cellular functions, including DNA damage responses (Phan and Dalla-Favera, 2004; Ranuncolo et al., 2007, 2008), signal transduction (Basso et al., 2010; Juszczynski et al., 2009), and cell cycle progression (Phan et al., 2005; Shaffer et al., 2000), it is possible that ABC-DLBCL cases carrying *BCL6* lesions have distinct phenotypic traits.

a benign lymphoproliferation. In contrast, *Blimp1*^{Cγ1}KO mice did not show reduced survival nor suffered from BALT-H (Figures S6C and S6D), suggesting that the BALT-H results from the expansion of *Blimp1*-deleted, extra-follicular mature B cells (see Table S4 for a comparison of the phenotypes from the two models). Taken together, these data provide conclusive evidence for *BLIMP1* as a bona fide tumor suppressor gene in ABC-DLBCL.

DISCUSSION

Heterogeneous Mechanisms of *BLIMP1* Inactivation

This study demonstrates that *BLIMP1* is inactivated in ABC-DLBCL through a variety of genetic means. In addition to truncating mutations and deletions, we describe a mechanism by which missense mutations inactivate BLIMP1 by either destabilizing the protein or impairing its transrepression activity. Moreover, we show that transcriptional silencing of *BLIMP1* via deregulating *BCL6* translocations represents an alternative mechanism to inactivate its function. The mutually exclusive nature of *BLIMP1* and *BCL6* lesions in DLBCL is consistent with the current model for plasma cell differentiation, whereby IRF4-mediated transcriptional repression of *BCL6* leads to derepression of *BLIMP1* and subsequent GC exit (Klein and Dalla-Favera, 2008; Saito et al., 2007); thus, structural alterations of either gene should play analogous roles in blocking terminal differentiation. Moreover, these

Despite IRF4 expression, one-third of ABC-DLBCLs lacked BLIMP1 protein expression in the absence of *BLIMP1* or *BCL6* structural alterations. Analysis of a limited number of cases ruled out the possibility that BLIMP1 promoter hypermethylation was responsible for the absence of Blimp1 expression, suggesting that additional unknown genetic lesions may contribute to blocking terminal differentiation. In our series, amplification of *SP1B* or *PAX5*, two genes that are also known to repress *BLIMP1* (Mora-Lopez et al., 2007; Schmidlin et al., 2008), did not seem to be involved (data not shown). However, genome-wide approaches may be necessary to determine whether structural alterations in other genes and/or microRNAs, such as those recently described to regulate *BLIMP1* expression (Leucci et al., 2010; Malumbres et al., 2009; Nie et al., 2008; West et al., 2009; Zhang et al., 2009), play a role in preventing BLIMP1 protein expression in this subset.

Association of *BLIMP1* Inactivation with Other Lesions

The long latency and the clonality of DLBCL in the *Blimp1* conditional-knockout mouse models indicate that oncogenic events affecting other pathways cooperate with *BLIMP1* inactivation to promote a full neoplastic phenotype and to cause DLBCL. Because the NF-κB transcriptional complex is known to be constitutively active in the majority of ABC-DLBCLs, genetic alterations within this pathway may be important contributors

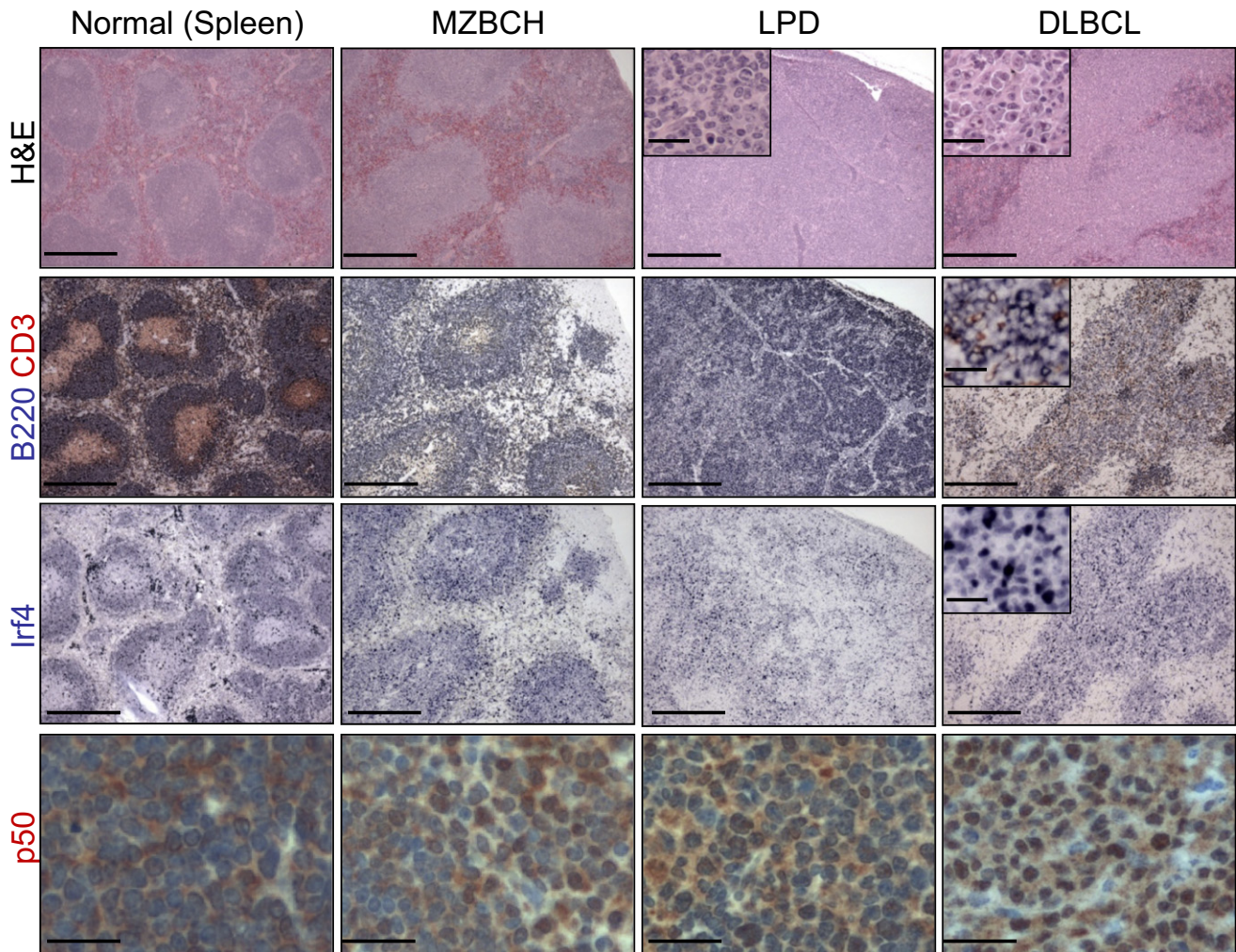


Figure 7. *Blimp1* B Cell Conditional Knockout Mice Develop DLBCL with an Activated Phenotype and Constitutive NF- κ B Activation

Representative spleen and lymph node sections from *Blimp1* knockout mice presenting with a spectrum of lymphoproliferative disorders, including MZBCH, LPD, and overt DLBCL, as compared to a wild-type control (see Results for a detailed histological description and Figure S6 for additional data). Tissues were stained with hematoxylin and eosin (H&E) or immunostained with antibodies against the B220 pan-B cell marker, IRF4, and the NF- κ B subunit p50, as indicated. Scale bar, 1250 μ m; inset, 125 μ m; scale is 50 μ m for p50 stain.

to lymphomagenesis. Interestingly, concurrent inactivation of *BLIMP1* and mutations within NF- κ B pathway components are found in a significant fraction of human ABC-DLBCLs (data not shown). Furthermore, the DLBCLs that develop in *Blimp1* conditional-knockout mice display evidence of constitutive NF- κ B activation. Thus, future in vivo studies should address the cooperative role of these two pathways in lymphomagenesis.

BLIMP1 as a Tumor Suppressor Gene

In the present study, we have provided converging evidence from human genetics, functional studies, and mouse models that *BLIMP1* is a bona fide tumor suppressor gene in ABC-DLBCL. One major role for *BLIMP1* inactivation in lymphomagenesis is to block terminal differentiation and to modulate the expression of genes involved in cell cycle progression. This notion is supported by our observation that introduction of *BLIMP1* into a DLBCL cell line leads to G1 cell cycle arrest, as

well as by previous work showing that activated *Blimp1* knockout mouse B cells have increased proliferative capacity (Shapiro-Shelef et al., 2003). Thus, the expansion of GC and non-GC MZ B cells observed in our mice may be in part due to the enhanced proliferation of *Blimp1*-null activated B cells failing to undergo terminal differentiation. The *Blimp1*^{CD19KO} and *Blimp1*^{C γ 1KO} mice will provide useful preclinical models to explore additional pathways contributing to lymphomagenesis.

EXPERIMENTAL PROCEDURES

Tumor Samples and Classification

Primary biopsies from 139 newly diagnosed patients with DLBCL were obtained from the archives of the Departments of Pathology at Columbia University and Weill Cornell Medical College, after approval by the respective Institutional Review Boards (Exempt Human Subject Research of anonymized/deidentified existing pathological specimens, under regulatory guideline 45 CFR 46.101(b)(4)). For a description of the 19 DLBCL cell lines used, see

Supplemental Experimental Procedures. Samples were classified by gene expression profile analysis into the ABC or GCB subtypes as previously described (Compagno et al., 2009). Cases that could not be profiled due to the lack of material or low percentage of tumor cells in the biopsy were classified into GC and non-GC DLBCL based on expression of CD10, BCL6, and IRF4 (Hans et al., 2004).

Mutational and Copy Number Analyses of the BLIMP1 Gene

Genomic DNA from 158 DLBCL samples was extracted according to standard methods and used for amplification of the *BLIMP1* coding exons as previously described (Pasqualucci et al., 2006). Purified amplicons were sequenced directly from both strands and compared to the corresponding germline sequence (NM_001198) using the Mutation Surveyor Version 2.41 software (Soft Genetics, State College, PA, USA). Mutations were confirmed on independent PCR products, and their somatic origin was verified by analysis of paired normal DNA, where available. In addition all mutations were verified in available databases of germline variants (NCBI dbSNP, Build 130; Ensembl; Watson genome sequence). Copy number analysis of *BLIMP1* was performed using a combination of fluorescent in situ hybridization, single nucleotide polymorphism profiling arrays using the Affymetrix Genome-Wide Human SNP Array 6.0 platform (Affymetrix, Santa Clara, CA, USA), and quantitative copy number PCR (see Supplemental Experimental Procedures for additional details).

Transient Transfections/Luciferase Reporter Assays

293T cells were transiently transfected with equimolar amounts (200 ng) of wild-type and mutant pCMV-HA-*BLIMP1* vectors via the calcium phosphate precipitation method, as described (Gu et al., 1993). For analysis of protein stability, transfected 293T cells were treated with 50 μ g/ml cycloheximide (Sigma-Aldrich) for 2, 4, and 8 hr before harvesting for protein analysis. For luciferase reporter assays, 293T cells were cotransfected with 10 ng wild-type or mutant pCMV-HA-*BLIMP1* vectors, 10 ng CIITA-Luc reporter construct, and 0.1 ng TK-RL Renilla reporter as control for transfection efficiency (Promega, Madison, WI, USA). Cells were harvested 48 hr after transfection, and the Dual Luciferase Reporter Assay (Promega) was performed according to the manufacturer's instructions, in three independent experiments.

Cell Proliferation and Cell Cycle Assays

Cellular proliferation was measured by an MTT assay (Roche) using 10,000 cells/well in duplicate in two independent experiments. To assess the cell cycle profile, 60 hr after infection with the indicated lentiviral supernatants, BJAB cells were labeled with bromodeoxyuridine (BrdU) for 30 min before harvesting. BrdU incorporation and DNA content were analyzed with the APC BrdU flow kit (Becton Dickinson) (see Supplemental Experimental Procedures for a detailed transduction protocol).

BCL6 Knockdown

A previously validated BCL6 lentiviral shRNA construct (Basso et al., 2010) was used to knockdown BCL6 expression in RCK8 B cells. Control and BCL6 shRNA lentiviruses were produced and transduced into RCK8 B cells as described. Twenty-four hours after the second round of infection, cells were selected with 1 μ g/ml puromycin for 5.5 days, and live cells were purified by MACS using the Dead Cell Removal Kit (Miltenyi Biotec, Auburn, CA, USA).

Ex Vivo Plasma Cell Differentiation Assay

Primary mouse B cells were purified from the spleen of 8 week old *Blimp1*^{CD19KO} mice using the Mouse B cell Isolation Kit (Miltenyi Biotec) and cultured in RPMI-1640 medium supplemented with 10% fetal calf serum, 100 U/ml penicillin, 100 U/ml streptomycin, 55 μ M β -mercaptoethanol, and 10 μ g/ml lipopolysaccharides (Sigma-Aldrich). For the complementation assay, cells were transduced after 1 day with PINCO retroviral vectors expressing wild-type HA-*BLIMP1* or its derivatives, as described. The percentage of CD138⁺ B220⁻ plasma cells in the transduced (GFP⁺) population was determined 48 and 72 hr after the second round of infection by flow cytometric analysis, using anti-CD138-APC (PharMingen, San Jose, CA, USA) and anti-B220-PerCP (PharMingen) antibodies. As control, splenic B cells from wild-type mice were treated in parallel with LPS and analyzed for differentiation 1 day earlier than transduced cells.

Mice

Blimp1^{CD19KO} and *Blimp1*^{C γ 1KO} mice and control littermates were generated on a mixed C57BL/6:129Sv background by crossing *Blimp1*^{fl/+} mice with *Blimp1*^{CD19HET} or *Blimp1*^{C γ 1HET} mice respectively, followed by offspring intercrossing. Genotyping was performed by PCR analysis, and the protocol is available upon request. Animals were monitored for tumor incidence and survival biweekly over a period of 10–18 months and sacrificed for analysis when visibly ill or at the end of the study, according to protocols approved by the Columbia University Institutional Animal Care and Use Committee. Flow cytometric analysis of B and T cell lymphoid compartments and histological examination of mouse tissues were also performed at 3, 12, and 15 months of age (n = 3–5 mice per genotype). A detailed description of the methods is available in the accompanying Supplemental Experimental Procedures. Kaplan-Meier event-free survival curves were generated using the GraphPad Prism 5 software (GraphPad Software, La Jolla, CA, USA), and statistical significance was calculated using the long-rank (Mantel-Cox) test. The Student's t test (unpaired, two-tailed) was used to assess whether differences in the incidence of lymphoproliferative disorders were significant in knockout mice compared to control wild-type littermates.

ACCESSION NUMBERS

The expression data reported in this paper have been deposited in the NCBI Gene Expression Omnibus (GEO) (<http://www.ncbi.nlm.nih.gov/geo>) database (Series Accession Number GSE12195).

SUPPLEMENTAL INFORMATION

Supplemental Information includes Supplemental Experimental Procedures, six figures, and four tables and can be found with this article online at doi:10.1016/j.ccr.2010.10.030.

ACKNOWLEDGMENTS

We thank U. Klein, D. Dominguez-Sola, and M. Saito for helpful discussions; A. Grunn for help with the sequencing analysis; J. Piskurich for providing the CIITA luciferase reporter; and G. Bornkamm for the bicistronic expression cassette. We also thank the Flow Cytometry, Transgenic Mouse and Genomics Shared Resources of the Herbert Irving Comprehensive Cancer Center. This work was supported by N.I.H. Grants CA-092625 and CA-37295, by a Specialized Center of Research grant from the Leukemia & Lymphoma Society, and by the Stewart Trust Fund. L.P. is on leave from the University of Perugia. The authors declare no conflicts of interest.

Received: April 15, 2010

Revised: July 28, 2010

Accepted: October 8, 2010

Published: December 13, 2010

REFERENCES

- Abramson, J.S., and Shipp, M.A. (2005). Advances in the biology and therapy of diffuse large B-cell lymphoma: moving toward a molecularly targeted approach. *Blood* 106, 1164–1174.
- Alizadeh, A.A., Eisen, M.B., Davis, R.E., Ma, C., Lossos, I.S., Rosenwald, A., Boldrick, J.C., Sabet, H., Tran, T., Yu, X., et al. (2000). Distinct types of diffuse large B-cell lymphoma identified by gene expression profiling. *Nature* 403, 503–511.
- Angelini-Duclos, C., Cattoretti, G., Lin, K.I., and Calame, K. (2000). Commitment of B lymphocytes to a plasma cell fate is associated with Blimp-1 expression in vivo. *J. Immunol.* 165, 5462–5471.
- Basso, K., Saito, M., Sumazin, P., Margolin, A.A., Wang, K., Lim, W.K., Kitagawa, Y., Schneider, C., Alvarez, M.J., Califano, A., and Dalla-Favera, R. (2010). Integrated biochemical and computational approach identifies BCL6 direct target genes controlling multiple pathways in normal germinal center B cells. *Blood* 115, 975–984.

- Casola, S., Cattoretti, G., Uyttersprot, N., Koralov, S.B., Seagal, J., Hao, Z., Waisman, A., Egert, A., Ghitza, D., and Rajewsky, K. (2006). Tracking germinal center B cells expressing germ-line immunoglobulin gamma1 transcripts by conditional gene targeting. *Proc. Natl. Acad. Sci. USA* *103*, 7396–7401.
- Cattoretti, G., Pasqualucci, L., Ballon, G., Tam, W., Nandula, S.V., Shen, Q., Mo, T., Murty, V.V., and Dalla-Favera, R. (2005). Deregulated BCL6 expression recapitulates the pathogenesis of human diffuse large B cell lymphomas in mice. *Cancer Cell* *7*, 445–455.
- Compagno, M., Lim, W.K., Grunn, A., Nandula, S.V., Brahmachary, M., Shen, Q., Bertoni, F., Ponzoni, M., Scandurra, M., Califano, A., et al. (2009). Mutations of multiple genes cause deregulation of NF-kappaB in diffuse large B-cell lymphoma. *Nature* *459*, 717–721.
- Davis, R.E., Brown, K.D., Siebenlist, U., and Staudt, L.M. (2001). Constitutive nuclear factor kappaB activity is required for survival of activated B cell-like diffuse large B cell lymphoma cells. *J. Exp. Med.* *194*, 1861–1874.
- Davis, R.E., Ngo, V.N., Lenz, G., Tolar, P., Young, R.M., Romesser, P.B., Kohlhammer, H., Lamy, L., Zhao, H., Yang, Y., et al. (2010). Chronic active B-cell-receptor signalling in diffuse large B-cell lymphoma. *Nature* *463*, 88–92.
- Falini, B., Fizzotti, M., Pucciarini, A., Bigerna, B., Marafioti, T., Gambacorta, M., Pacini, R., Alunni, C., Natali-Tanci, L., Ugolini, B., et al. (2000). A monoclonal antibody (MUM1p) detects expression of the MUM1/IRF4 protein in a subset of germinal center B cells, plasma cells, and activated T cells. *Blood* *95*, 2084–2092.
- Gaidano, G., Hauptschein, R.S., Parsa, N.Z., Offit, K., Rao, P.H., Lenoir, G., Knowles, D.M., Chaganti, R.S., and Dalla-Favera, R. (1992). Deletions involving two distinct regions of 6q in B-cell non-Hodgkin lymphoma. *Blood* *80*, 1781–1787.
- Gu, W., Cechova, K., Tassi, V., and Dalla-Favera, R. (1993). Opposite regulation of gene transcription and cell proliferation by c-Myc and Max. *Proc. Natl. Acad. Sci. USA* *90*, 2935–2939.
- Hans, C.P., Weisenburger, D.D., Greiner, T.C., Gascoyne, R.D., Delabie, J., Ott, G., Muller-Hermelink, H.K., Campo, E., Braziel, R.M., Jaffe, E.S., et al. (2004). Confirmation of the molecular classification of diffuse large B-cell lymphoma by immunohistochemistry using a tissue microarray. *Blood* *103*, 275–282.
- Huang, J.Z., Sanger, W.G., Greiner, T.C., Staudt, L.M., Weisenburger, D.D., Pickering, D.L., Lynch, J.C., Armitage, J.O., Warnke, R.A., Alizadeh, A.A., et al. (2002). The t(14;18) defines a unique subset of diffuse large B-cell lymphoma with a germinal center B-cell gene expression profile. *Blood* *99*, 2285–2290.
- Iqbal, J., Sanger, W.G., Horsman, D.E., Rosenwald, A., Pickering, D.L., Dave, B., Dave, S., Xiao, L., Cao, K., Zhu, Q., et al. (2004). BCL2 translocation defines a unique tumor subset within the germinal center B-cell-like diffuse large B-cell lymphoma. *Am. J. Pathol.* *165*, 159–166.
- Iqbal, J., Greiner, T.C., Patel, K., Dave, B.J., Smith, L., Ji, J., Wright, G., Sanger, W.G., Pickering, D.L., Jain, S., et al. (2007). Distinctive patterns of BCL6 molecular alterations and their functional consequences in different subgroups of diffuse large B-cell lymphoma. *Leukemia* *21*, 2332–2343.
- Juszczynski, P., Chen, L., O'Donnell, E., Polo, J.M., Ranuncolo, S.M., Dalla-Favera, R., Melnick, A., and Shipp, M.A. (2009). BCL6 modulates tonic BCR signaling in diffuse large B-cell lymphomas by repressing the SYK phosphatase, PTPROt. *Blood* *114*, 5315–5321.
- Klein, U., and Dalla-Favera, R. (2008). Germinal centres: role in B-cell physiology and malignancy. *Nat. Rev. Immunol.* *8*, 22–33.
- Klein, U., Casola, S., Cattoretti, G., Shen, Q., Lia, M., Mo, T., Ludwig, T., Rajewsky, K., and Dalla-Favera, R. (2006). Transcription factor IRF4 controls plasma cell differentiation and class-switch recombination. *Nat. Immunol.* *7*, 773–782.
- Lenz, G., Davis, R.E., Ngo, V.N., Lam, L., George, T.C., Wright, G.W., Dave, S.S., Zhao, H., Xu, W., Rosenwald, A., et al. (2008a). Oncogenic CARD11 mutations in human diffuse large B cell lymphoma. *Science* *319*, 1676–1679.
- Lenz, G., Wright, G.W., Emre, N.C., Kohlhammer, H., Dave, S.S., Davis, R.E., Carty, S., Lam, L.T., Shaffer, A.L., Xiao, W., et al. (2008b). Molecular subtypes of diffuse large B-cell lymphoma arise by distinct genetic pathways. *Proc. Natl. Acad. Sci. USA* *105*, 13520–13525.
- Leucci, E., Onnis, A., Cocco, M., De Falco, G., Imperatore, F., Giuseppina, A., Costanzo, V., Cerino, G., Mannucci, S., Cantisani, R., et al. (2010). B-cell differentiation in EBV-positive Burkitt lymphoma is impaired at posttranscriptional level by miRNA-altered expression. *Int. J. Cancer* *126*, 1316–1326.
- Lin, Y., Wong, K., and Calame, K. (1997). Repression of c-myc transcription by Blimp-1, an inducer of terminal B cell differentiation. *Science* *276*, 596–599.
- Malumbres, R., Sarosiek, K.A., Cubedo, E., Ruiz, J.W., Jiang, X., Gascoyne, R.D., Tibshirani, R., and Lossos, I.S. (2009). Differentiation stage-specific expression of microRNAs in B lymphocytes and diffuse large B-cell lymphomas. *Blood* *113*, 3754–3764.
- Monti, S., Savage, K.J., Kutok, J.L., Feuerhake, F., Kurtin, P., Mihm, M., Wu, B., Pasqualucci, L., Neuberger, D., Aguiar, R.C., et al. (2005). Molecular profiling of diffuse large B-cell lymphoma identifies robust subtypes including one characterized by host inflammatory response. *Blood* *105*, 1851–1861.
- Mora-Lopez, F., Reales, E., Brieva, J.A., and Campos-Caro, A. (2007). Human BSAP and BLIMP1 conform an autoregulatory feedback loop. *Blood* *110*, 3150–3157.
- Morin, R.D., Johnson, N.A., Severson, T.M., Mungall, A.J., An, J., Goya, R., Paul, J.E., Boyle, M., Woolcock, B.W., Kuchenbauer, F., et al. (2010). Somatic mutations altering EZH2 (Tyr641) in follicular and diffuse large B-cell lymphomas of germinal-center origin. *Nat. Genet.* *42*, 181–185.
- Nie, K., Gomez, M., Landgraf, P., Garcia, J.F., Liu, Y., Tan, L.H., Chadburn, A., Tuschl, T., Knowles, D.M., and Tam, W. (2008). MicroRNA-mediated down-regulation of PRDM1/Blimp-1 in Hodgkin/Reed-Sternberg cells: a potential pathogenetic lesion in Hodgkin lymphomas. *Am. J. Pathol.* *173*, 242–252.
- Ohinata, Y., Payer, B., O'Carroll, D., Ancelin, K., Ono, Y., Sano, M., Barton, S.C., Obukhanych, T., Nussenzweig, M., Tarakhovskiy, A., et al. (2005). Blimp1 is a critical determinant of the germ cell lineage in mice. *Nature* *436*, 207–213.
- Pasqualucci, L., Migliazza, A., Basso, K., Houldsworth, J., Chaganti, R.S., and Dalla-Favera, R. (2003). Mutations of the BCL6 proto-oncogene disrupt its negative autoregulation in diffuse large B-cell lymphoma. *Blood* *101*, 2914–2923.
- Pasqualucci, L., Compagno, M., Houldsworth, J., Monti, S., Grunn, A., Nandula, S.V., Aster, J.C., Murty, V.V., Shipp, M.A., and Dalla-Favera, R. (2006). Inactivation of the PRDM1/BLIMP1 gene in diffuse large B cell lymphoma. *J. Exp. Med.* *203*, 311–317.
- Phan, R.T., and Dalla-Favera, R. (2004). The BCL6 proto-oncogene suppresses p53 expression in germinal-centre B cells. *Nature* *432*, 635–639.
- Phan, R.T., Saito, M., Basso, K., Niu, H., and Dalla-Favera, R. (2005). BCL6 interacts with the transcription factor Miz-1 to suppress the cyclin-dependent kinase inhibitor p21 and cell cycle arrest in germinal center B cells. *Nat. Immunol.* *6*, 1054–1060.
- Piskurich, J.F., Lin, K.I., Lin, Y., Wang, Y., Ting, J.P., and Calame, K. (2000). BLIMP-1 mediates extinction of major histocompatibility class II transactivator expression in plasma cells. *Nat. Immunol.* *1*, 526–532.
- Ranuncolo, S.M., Polo, J.M., and Melnick, A. (2008). BCL6 represses CHEK1 and suppresses DNA damage pathways in normal and malignant B-cells. *Blood Cells Mol. Dis.* *41*, 95–99.
- Ranuncolo, S.M., Polo, J.M., Dierov, J., Singer, M., Kuo, T., Grealley, J., Green, R., Carroll, M., and Melnick, A. (2007). Bcl-6 mediates the germinal center B cell phenotype and lymphomagenesis through transcriptional repression of the DNA-damage sensor ATR. *Nat. Immunol.* *8*, 705–714.
- Rickert, R.C., Roes, J., and Rajewsky, K. (1997). B lymphocyte-specific, Cre-mediated mutagenesis in mice. *Nucleic Acids Res.* *25*, 1317–1318.
- Rosenwald, A., Wright, G., Leroy, K., Yu, X., Gaulard, P., Gascoyne, R.D., Chan, W.C., Zhao, T., Haioun, C., Greiner, T.C., et al. (2003). Molecular diagnosis of primary mediastinal B cell lymphoma identifies a clinically favorable subgroup of diffuse large B cell lymphoma related to Hodgkin lymphoma. *J. Exp. Med.* *198*, 851–862.
- Saito, M., Gao, J., Basso, K., Kitagawa, Y., Smith, P.M., Bhagat, G., Pernis, A., Pasqualucci, L., and Dalla-Favera, R. (2007). A signaling pathway mediating

- downregulation of BCL6 in germinal center B cells is blocked by BCL6 gene alterations in B cell lymphoma. *Cancer Cell* 12, 280–292.
- Savage, K.J., Monti, S., Kutok, J.L., Cattoretti, G., Neuberg, D., De Leval, L., Kurtin, P., Dal Cin, P., Ladd, C., Feuerhake, F., et al. (2003). The molecular signature of mediastinal large B-cell lymphoma differs from that of other diffuse large B-cell lymphomas and shares features with classical Hodgkin lymphoma. *Blood* 102, 3871–3879.
- Schmidlin, H., Diehl, S.A., Nagasawa, M., Scheeren, F.A., Schotte, R., Uittenbogaart, C.H., Spits, H., and Blom, B. (2008). Spi-B inhibits human plasma cell differentiation by repressing BLIMP1 and XBP-1 expression. *Blood* 112, 1804–1812.
- Shaffer, A.L., Rosenwald, A., and Staudt, L.M. (2002a). Lymphoid malignancies: the dark side of B-cell differentiation. *Nat. Rev. Immunol.* 2, 920–932.
- Shaffer, A.L., Lin, K.I., Kuo, T.C., Yu, X., Hurt, E.M., Rosenwald, A., Giltnane, J.M., Yang, L., Zhao, H., Calame, K., and Staudt, L.M. (2002b). Blimp-1 orchestrates plasma cell differentiation by extinguishing the mature B cell gene expression program. *Immunity* 17, 51–62.
- Shaffer, A.L., Yu, X., He, Y., Boldrick, J., Chan, E.P., and Staudt, L.M. (2000). BCL-6 represses genes that function in lymphocyte differentiation, inflammation, and cell cycle control. *Immunity* 13, 199–212.
- Shapiro-Shelef, M., Lin, K.I., McHeyzer-Williams, L.J., Liao, J., McHeyzer-Williams, M.G., and Calame, K. (2003). Blimp-1 is required for the formation of immunoglobulin secreting plasma cells and pre-plasma memory B cells. *Immunity* 19, 607–620.
- Sunyaev, S., Ramensky, V., Koch, I., Lathe, W., 3rd, Kondrashov, A.S., and Bork, P. (2001). Prediction of deleterious human alleles. *Hum. Mol. Genet.* 10, 591–597.
- Tam, W., Gomez, M., Chadburn, A., Lee, J.W., Chan, W.C., and Knowles, D.M. (2006). Mutational analysis of PRDM1 indicates a tumor-suppressor role in diffuse large B-cell lymphomas. *Blood* 107, 4090–4100.
- Tunayapin, C., Shaffer, A.L., Angelin-Duclos, C.D., Yu, X., Staudt, L.M., and Calame, K.L. (2004). Direct repression of prdm1 by Bcl-6 inhibits plasmacytic differentiation. *J. Immunol.* 173, 1158–1165.
- West, J.A., Viswanathan, S.R., Yabuuchi, A., Cunniff, K., Takeuchi, A., Park, I.H., Sero, J.E., Zhu, H., Perez-Atayde, A., Frazier, A.L., et al. (2009). A role for Lin28 in primordial germ-cell development and germ-cell malignancy. *Nature* 460, 909–913.
- Ye, B.H., Lista, F., Lo Coco, F., Knowles, D.M., Offit, K., Chaganti, R.S., and Dalla-Favera, R. (1993). Alterations of a zinc finger-encoding gene, BCL-6, in diffuse large-cell lymphoma. *Science* 262, 747–750.
- Ye, B.H., Chaganti, S., Chang, C.C., Niu, H., Corradini, P., Chaganti, R.S., and Dalla-Favera, R. (1995). Chromosomal translocations cause deregulated BCL6 expression by promoter substitution in B cell lymphoma. *EMBO J.* 14, 6209–6217.
- Zhang, J., Jima, D.D., Jacobs, C., Fischer, R., Gottwein, E., Huang, G., Lugar, P.L., Lagoo, A.S., Rizzieri, D.A., Friedman, D.R., et al. (2009). Patterns of microRNA expression characterize stages of human B-cell differentiation. *Blood* 113, 4586–4594.